

Vibrating-Coil Magnetometry of the Spin Liquid Properties of $\text{Tb}_2\text{Ti}_2\text{O}_7$

S. Legl,¹ C. Krey,¹ S. R. Dunsiger,¹ H. A. Dabkowska,² J. A. Rodriguez,^{3,4} G. M. Luke,³ and C. Pfleiderer¹

¹Physik-Department E21, Technische Universität München, D-85748 Garching, Germany

²Brockhouse Institute for Materials Research, McMaster University, Hamilton, Ontario L8S 4M1, Canada

³Department of Physics and Astronomy, McMaster University, Hamilton, Ontario L8S 4M1, Canada

⁴Laboratory for Muon Spin Spectroscopy, Paul Scherrer Institut, 5232 Villigen, Switzerland

(Received 10 January 2012; published 23 July 2012)

We have explored the spin liquid state in $\text{Tb}_2\text{Ti}_2\text{O}_7$ with vibrating-coil magnetometry down to ~ 0.04 K under magnetic fields up to 5 T. We observe magnetic history dependence below $T^* \sim 0.2$ K reminiscent of the classical spin ice systems $\text{Ho}_2\text{Ti}_2\text{O}_7$ and $\text{Dy}_2\text{Ti}_2\text{O}_7$. The magnetic phase diagram inferred from the magnetization is essentially isotropic, without evidence of magnetization plateaus as anticipated for so-called quantum spin ice, predicted theoretically for [111] when quantum fluctuations renormalize the interactions. Instead, the magnetization for $T \ll T^*$ agrees semiquantitatively with the predictions of “all-in–all-out” (AIAO) antiferromagnetism. Taken together, this suggests that the spin liquid state in $\text{Tb}_2\text{Ti}_2\text{O}_7$ is akin to an incipient AIAO antiferromagnet.

DOI: [10.1103/PhysRevLett.109.047201](https://doi.org/10.1103/PhysRevLett.109.047201)

PACS numbers: 75.30.Kz, 75.40.Cx, 75.40.Gb, 75.60.Ej

Pyrochlore oxides, $A_2B_2O_7$, in which rare earth magnetic moments are located on the A site of a three-dimensional network of corner sharing tetrahedra are model systems of geometric frustration [1]. The consequences of such geometric frustration are intimately connected with the nature of the magnetic anisotropy at the rare earth site. For instance, in $\text{Ho}_2\text{Ti}_2\text{O}_7$ and $\text{Dy}_2\text{Ti}_2\text{O}_7$ a strong easy-axis (Ising) anisotropy along the local [111] axis in the unit cell, together with net ferromagnetic interactions, are the most important preconditions for the emergence of the highly celebrated spin ice behavior [2–5].

A major unresolved question in geometric frustration concerns the fate of the spin ice state, when the strength of the local Ising anisotropy is reduced. This may boost the relative importance of quantum fluctuations. In fact, an exciting theoretical proposal states that quantum fluctuations may renormalize the exchange interactions of an unfrustrated $\langle 111 \rangle$ Ising antiferromagnet, making them effectively ferromagnetic. The associated novel state is referred to as quantum spin ice (QSI) [6–8] and may be viewed as a spin liquid in which thermal longitudinal spin fluctuations, which break the spin ice rules, as well as thermal and quantum fluctuations transverse to the local $\langle 111 \rangle$ directions are relevant. Compelling evidence of a QSI would be magnetization plateaus like those observed in $\text{Ho}_2\text{Ti}_2\text{O}_7$ and $\text{Dy}_2\text{Ti}_2\text{O}_7$, for a magnetic field strictly along a global $\langle 111 \rangle$ axis [9–12]. In turn, an anisotropy of the magnetic phase diagram would be expected, reminiscent of classical spin ice. Note, however, that this use of the term “quantum spin ice” differs from that associated with isostructural compounds like $\text{Yb}_2\text{Ti}_2\text{O}_7$ [13], where the crystal field anisotropy is XY-like in character [14].

An ideal model system to study whether any of the classical spin ice properties survive under reduced local magnetic anisotropy is $\text{Tb}_2\text{Ti}_2\text{O}_7$. At high temperatures $\text{Tb}_2\text{Ti}_2\text{O}_7$

exhibits a Curie-Weiss susceptibility with a large effective moment $\mu_{\text{eff}} = 9.6 \mu_B \text{Tb}^{-1}$ and a negative Curie-Weiss temperature Θ_{CW} characteristic of antiferromagnetic interactions [15,16]. As the crystal electric field (CEF) of the Tb^{3+} ion leads to a ground state doublet and an energy gap of ~ 18 K to the first excited state [16,17], antiferromagnetic order is expected around ~ 1 K [18]. Surprisingly however, μSR [15,19], the ac susceptibility [18,20], and neutron spin echo [20,21] established strong spin dynamics down to 20 mK without signs of long-range magnetic order.

The origin and nature of the lack of long-range magnetic order in $\text{Tb}_2\text{Ti}_2\text{O}_7$ represents a major puzzle in geometrically frustrated magnetism. It must, however, be a sensitive function of the low lying energy levels. X-ray diffraction [22] and a related transition at ~ 0.15 K [23] suggest a cooperative Jahn-Teller distortion. A possible splitting of the doublet to yield a singlet ground state has been inferred from specific heat data [24] and modeled [25], though this is at odds with high energy resolution neutron scattering [26]. The large electronic-nuclear hyperfine coupling of Tb suggests that nuclear degrees of freedom may also be important. It is unresolved if evidence for magnetic glassiness in the milli-Kelvin regime is intrinsic [27] or due to defects [20,28]. Moreover, for magnetic fields applied along $\langle 110 \rangle$, the specific heat [29] and neutron scattering [30] suggest field-induced order with spin-ice like properties [31–33], while the spin order for fields along $\langle 111 \rangle$ is undetermined [34]. Magnetoelastic effects are also known to be very pronounced [22,35,36], consistent with the observation of pressure induced antiferromagnetic order [37].

Calculations exploring the role of the interaction strength and CEF splitting suggest that $\text{Tb}_2\text{Ti}_2\text{O}_7$ is at the border between a QSI and “all-in–all-out” (AIAO) antiferromagnetism [6–8]. However, because the zero-frequency QSI correlations may be masked by strong fluctuations and

difficult to detect experimentally, it has been emphasized that magnetization measurements at mK temperatures are ideal to identify a QSI, since they probe the zero frequency and zero wave vector response.

The existence of QSI in $\text{Tb}_2\text{Ti}_2\text{O}_7$ has been addressed by Baker *et al.* [38], who infer the existence of magnetization plateaus from ac susceptibility data down to 25 mK, as well as μSR measurements which exhibit peaks and kinks in the spin lattice relaxation rate. In another study, Lhotel *et al.* [39] recently report extraction magnetometry and ac susceptibility down to 80 mK claiming the absence of magnetization plateaus. However, data reported in the former study probe the response at *finite* frequency, while the latter study does not extend to low enough temperatures to be conclusive. Moreover, extraction magnetometry suffers from the risk of tiny sample vibrations in the magnetic field, thereby changing the field history of the sample. The former and the latter study address the $\langle 111 \rangle$, and the $\langle 111 \rangle$ and $\langle 110 \rangle$ direction, respectively. Taken together, the nature of the spin liquid state in $\text{Tb}_2\text{Ti}_2\text{O}_7$ and the proposal of QSI are, hence, unresolved.

In this Letter, we address, to the best of our knowledge, for the first time the properties of $\text{Tb}_2\text{Ti}_2\text{O}_7$ and the possible existence of QSI down to sufficiently low temperatures under conditions avoiding parasitic modifications of the field history. The magnetization of a $\text{Tb}_2\text{Ti}_2\text{O}_7$ single crystal was measured at Technische Universität München using a bespoke vibrating-coil magnetometer (VCM) for temperatures down to ~ 0.04 K and magnetic fields up to 5 T [40,41]. Our VCM represents a new development previously thought to be prohibitively difficult. As the main advantage of the VCM, the sample does not move during measurements (the detection system is completely decoupled from the dilution refrigerator). The coil set was operated at 36.5 Hz, and the sample temperature was monitored with several RuO_2 and Speer sensors. Great care was taken to ensure good thermal anchoring (for details, see [41]).

Magnetic field sweeps at up to 1 T were recorded in a step mode, where the field was kept constant while recording the magnetization. Magnetization data up to 5 T were recorded while sweeping the magnetic field continuously at 15 mT min^{-1} . For studies of a $\langle 100 \rangle$ and $\langle 110 \rangle$ direction, the sample was mounted on a small copper wedge, and the orientation confirmed with Laue x-ray diffraction. The empty sample holder was measured to determine the background signal. The VCM data recorded below 1.5 K were calibrated by means of a Ni standard and the extrapolated magnetization of the $\text{Tb}_2\text{Ti}_2\text{O}_7$ sample as measured at 1.8 K in a Quantum Design magnetic property measurement system. High temperature data were recorded in an Oxford Instruments vibrating sample magnetometer.

For our study, a single crystal was grown at McMaster University by optical float zoning. The feed and seed rods were prepared by annealing high-purity Tb_4O_7 and TiO_2 in air. The sample was then float zoned in a high-purity

Ar atmosphere of 4 bar with a rate of 7 mm h^{-1} [42]. Powder x-ray diffraction confirmed that the ingot was phase pure with the correct crystal structure. A single-crystalline disk ($7 \times 4.1 \times 0.8 \text{ mm}^3$) was cut from the ingot for the magnetization measurements. The disk was oriented perpendicular to a $\langle 111 \rangle$ direction within $\sim 1^\circ$. The magnetic properties of this crystal as recorded above ~ 1.5 K were in excellent agreement with the literature. Interestingly, the strongly field-dependent specific heat anomaly reported by Hamaguchi *et al.* [43] was recently identified as a parasitic effect [44]. Even though we did not measure the specific heat data of our sample, the absence of any anomalies in dM/dT , representing by Maxwells relations the magnetocaloric effect dS/dB , strongly suggests the absence of such a specific heat anomaly and thus an excellent sample quality.

Demagnetizing fields were corrected for the [111] orientation, approximating our sample as an ellipsoid with a demagnetizing factor $N = 0.34$. As we will show, the conclusions drawn from our data for [100] and [110] do not depend on this correction, so only raw data as a function of applied field are shown. The internal fields were estimated to deviate by a few degrees from the [100] and [110] directions because the plane of the disk was tilted with respect to the applied field. In addition, the demagnetization fields in the tilted sample may have been slightly inhomogeneous.

Figure 1 illustrates the temperature dependence of the magnetization in an applied field of 10 mT, where data for [100] and [110] have been shifted by $0.03 \mu_B \text{ Tb}^{-1}$ and $0.06 \mu_B \text{ Tb}^{-1}$, respectively, for clarity (the uncertainty in the constant background is $\sim \pm 0.015 \mu_B \text{ Tb}^{-1}$). Prior to recording these data, the superconducting magnet was demagnetized at ~ 2.3 K to remove any parasitic remanent fields. After zero-field cooling the field was increased at

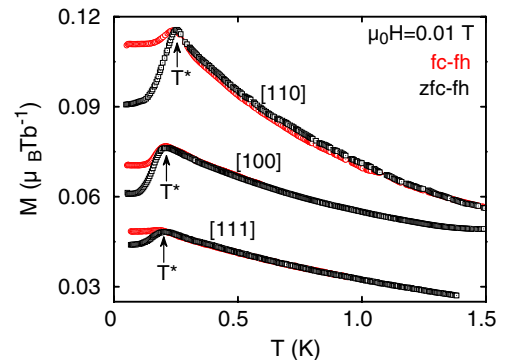


FIG. 1 (color online). Temperature dependence of the magnetization of $\text{Tb}_2\text{Ti}_2\text{O}_7$ in a small applied magnetic field of 10 mT. Below $T^* \sim 200$ mK a distinct difference between data recorded under zero-field cooling (zfc) and field cooling (fc) emerges, characteristic of a glassy magnetic state (all data were recorded while field heating (fh) to minimize systematic errors). Curves are shifted for clarity as described in the text.

a rate of 1 mT min^{-1} to the set point of 10 mT and data recorded while heating the sample continuously at 5 mK min^{-1} up to $\sim 1.5 \text{ K}$ (zfc-fh). Following this, the sample was cooled down with the field unchanged and data recorded while heating at the same rate (fc-fh).

With decreasing temperature the magnetization increases with a positive curvature consistent with the paramagnetic properties at high temperatures. In all field directions, the curves display a cusp in the zfc-fh and fc-fh data. We find slightly different values of $T^* \sim 0.246$, ~ 0.212 , and $\sim 0.204 \text{ K}$ for [110], [100], and [111], respectively, not reported previously. For $T > T^*$ the zfc-fh and fc-fh data agree essentially (the tiny difference for [110] is most likely associated with a small drift of the detection system).

The shape of the cusp, the absolute difference of zfc-fh and fc-fh data, and the qualitative temperature dependence of the data provide strong evidence of the emergence of intrinsic magnetic glassiness below T^* , which is essentially isotropic. Note that magnetic ordering coexisting with persistent low temperature fluctuations has been reported in a variety of geometrically frustrated systems [45,46]. It is, therefore, perfectly consistent with the persistent muon spin relaxation observed in $\text{Tb}_2\text{Ti}_2\text{O}_7$ [15,19,23]. The absolute size of the magnetization for $T > T^*$, being largest for [110] and smallest for [111], suggests that the tiny variation in T^* and the difference between fc-fh and zfc-fh, which are also largest for [110] and smallest for [111], originate from the magnetic anisotropy. However, in comparison to simple cubic systems the anisotropy is unusual, as [110] cannot be a soft direction.

Presented in Figs. 2(a)–2(d) are magnetization data in the range from ~ 0.043 to $\sim 50 \text{ K}$ under magnetic fields up to 5 T for [110], [100], and [111], respectively. Data below 1 K were recorded after zero-field cooling. For the field and temperature scale shown in Fig. 2 field-cooled data are analogous. Note that panel (d) shows the data of panel (c) as a function of calculated internal field. Apart from a shift of the characteristic features in the magnetization towards lower fields, demagnetizing fields do not affect our conclusions. The linear magnetic field dependence at $\sim 50 \text{ K}$ becomes highly nonlinear at the lowest temperatures studied. It remains unsaturated at 5 T , even though the magnetization reaches a large value between 5 and $6 \mu_B \text{ Tb}^{-1}$.

On the scale shown in Fig. 2, we find no evidence for a magnetization plateau, predicted for QSI. This contrasts with classical spin ice systems, where the magnetization plateaus are a prominent feature, for magnetic fields applied strictly along $\langle 111 \rangle$ for similar values of the magnetization. Moreover, we observe some fine structure in $dM/d\mu_0 H$ not reported before [Figs. 2(e)–2(h)]. Namely, for the lowest temperature the calculated first derivatives allow us to define two crossover scales $\mu_0 H_1$ and $\mu_0 H_2$. The field $\mu_0 H_1$ marks the end of the initial rise of the magnetization associated with the initial drop of $dM/d\mu_0 H$,

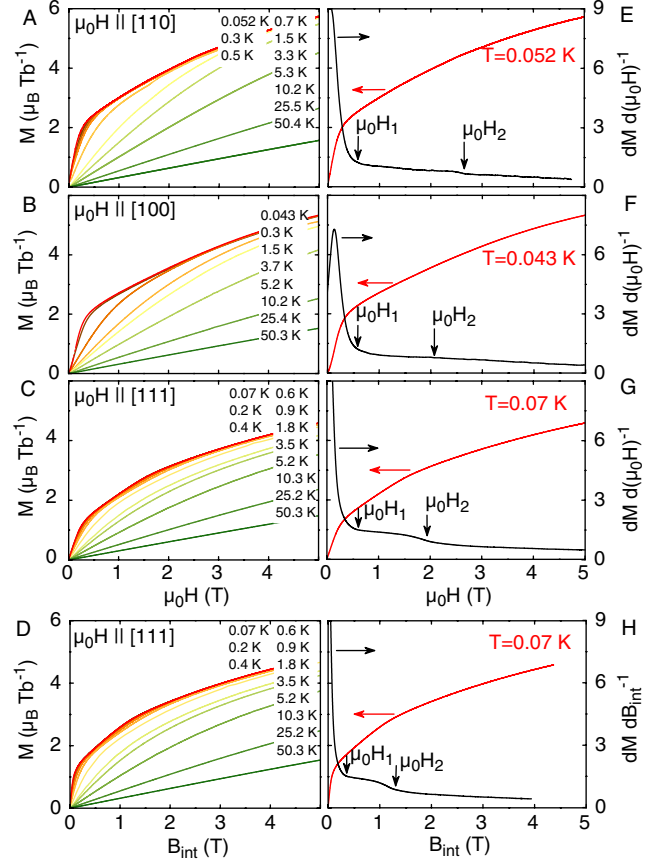


FIG. 2 (color online). Magnetization of $\text{Tb}_2\text{Ti}_2\text{O}_7$ for temperatures in the range ~ 0.043 to $\sim 50 \text{ K}$ under magnetic fields up to 5 T . Data below 1 K were recorded after zfc. Panels (a), (b), and (c) display data as a function of the applied field along [110], [100], and [111]. Panel (d) shows the data of panel (c) as a function of internal field. Panels (e), (f), (g), and (h) show the numerical derivative of the experimental data recorded at the lowest temperatures in order to illustrate the definition of the characteristic fields $\mu_0 H_1$ and $\mu_0 H_2$.

while $\mu_0 H_2 > \mu_0 H_1$ marks a faint drop of $dM/d\mu_0 H$. Thus, the magnetization for $\mu_0 H_1 < B < \mu_0 H_2$ cannot correspond to a plateau (or remnants thereof), since the slope decreases when exceeding $\mu_0 H_2$ without a point of inflection at $\mu_0 H_2$. In addition, $\mu_0 H_1$ and $\mu_0 H_2$ exist for all directions and are not specific for [111].

Corroborating evidence of the characteristic energy scales $\mu_0 H_1$ and $\mu_0 H_2$ may have been seen in time-of-flight neutron scattering for field parallel $\langle 110 \rangle$, where the scattering condenses into a new Bragg peak around $\mu_0 H_1$ consistent with a polarized paramagnet [30]. A magnetically ordered phase, which supports spin wave excitations, is induced around $\mu_0 H_2$, consistent with crossover phenomena found in the specific heat and ac susceptibility [30]. Above $\mu_0 H_2$ magnetization plateaus are thus no longer expected.

Shown in Fig. 3(a) are typical zero-field cooled magnetization data for the [111] direction in smaller

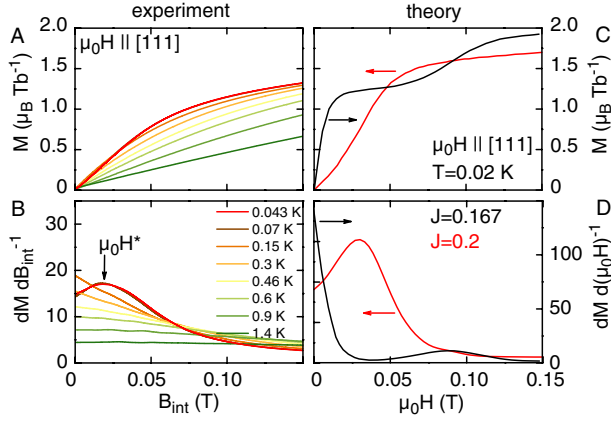


FIG. 3 (color online). Experimental and theoretical low-field magnetization of $\text{Tb}_2\text{Ti}_2\text{O}_7$ for the [111] axis in the parameter range of the predicted magnetization plateau of quantum spin ice. Only zero-field cooled data are shown. (a) Magnetic field dependence of the magnetization of $\text{Tb}_2\text{Ti}_2\text{O}_7$ in small fields at various temperatures. (b) Numerical derivative of the data shown in panel (a). (c) Theoretically predicted magnetization for a quantum spin ice state in $\text{Tb}_2\text{Ti}_2\text{O}_7$ as reported in Ref. [8]. (d) Derivative of the theoretical data shown in panel (c).

applied fields, where we find no evidence of magnetization plateaus either. Qualitatively field-cooled data are the same, as shown in the Supplemental Material [47]. The absence of magnetization plateaus is most evident in dM/dB_{int} calculated from the data shown in Fig. 3(b). This plot does not display a point of inflection of $M(B_{\text{int}})$. Instead, dM/dB_{int} has a broad maximum only. Data for [110] and [100] shown in the Supplemental Material [47] are similar to [111]. Our data are thereby consistent with Ref. [39], but extend a factor of 2 lower in temperature, well into the proposed QSI regime.

For comparison with the experimental data, we reproduce in Figs. 3(c) and 3(d) theoretical calculations of the magnetization and their first derivatives at 20 mK for $J = 0.167$ (QSI) and $J = 0.2$ (AIAO) [8]. The most important qualitative difference concerns the marked change in the slope of $dM/d\mu_0H$ at low field (< 0.05 T) from negative to positive for QSI and AIAO structures, respectively. Notice that experimentally dM/dB_{int} at 43 and 70 mK has a positive slope at low field and a maximum at 0.03 T. This observation is independent of the field history as described above.

However, the calculated AIAO spin state is based on a CEF splitting $1/\Delta$, which is reduced by a factor of 2 as compared with experiment and an exchange coupling, $J = 0.2$, that is larger than that inferred experimentally through examination of the magnetization and ac susceptibility above 8 K in terms of the CEF scheme in the mean field approximation [16]. Unfortunately, we cannot offer an explanation for the discrepancy of the CEF splitting. As for the exchange coupling it is important to realize that differing values have been extracted in low and high fields and

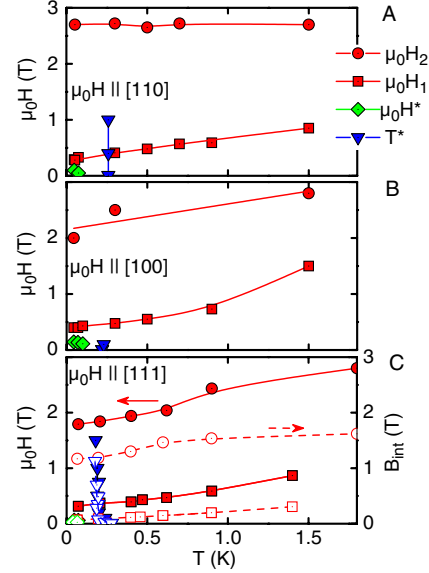


FIG. 4 (color online). Magnetic phase diagram of $\text{Tb}_2\text{Ti}_2\text{O}_7$ for [110], [100], and [111] as inferred from the magnetization. The crossover fields μ_0H_1 and μ_0H_2 are larger the magnetically softer the direction. This may serve as a testing ground for the validity of theoretical models. Open symbols in panel (c) correspond to the phase diagram after correction of demagnetizing effects.

the associated analysis is only considered valid in the paramagnetic regime [16]. Note that the theoretically predicted ground state depends on the model used and its implementation [7,48]. For example, as shown in Ref. [7], assuming $J_{\text{ex}} = 1/6$ K [7,48,49], the dipolar spin ice model and a cubic unit cell model with Ewald summed dipole-dipole interactions and CEFs predict AIAO antiferromagnetism and long-range spin ice with ordering wave vector $\vec{q} = (000)$, LRSI_{000} , respectively. In particular, the model of Refs. [6–8] completely ignores the possibility of anisotropic exchange and higher multipolar couplings. Because $\text{Tb}_2\text{Ti}_2\text{O}_7$ does not develop spontaneous long-range magnetic order, it seems natural to conclude that the spin liquid in $\text{Tb}_2\text{Ti}_2\text{O}_7$ is dominated by strong fluctuations at the border of AIAO antiferromagnetism. This may be referred to as incipient AIAO antiferromagnetism, supported by the nearly isotropic magnetic phase diagrams shown in Fig. 4. Note that the open symbols in panel (c) show the phase diagram when correcting demagnetizing effects. The expected corrections in panels (a) and (b) are smaller than for panel (c). As a function of magnetic field, we find two crossover scales μ_0H_1 and μ_0H_2 , where neutron scattering suggests different changes of the underlying microscopic properties [30].

In conclusion, we find no evidence of the magnetization plateaus in $\text{Tb}_2\text{Ti}_2\text{O}_7$ expected of QSI and fluctuation-induced ferromagnetic interactions. Instead, our data are in semiquantitative agreement with the theoretical predictions of AIAO antiferromagnetism, suggesting that the spin liquid state in $\text{Tb}_2\text{Ti}_2\text{O}_7$ may be viewed as an incipient

AIAO antiferromagnet. Generally, below ~ 100 mK, a positive slope followed by a maximum in dM/dB in low fields must be reproduced by any future theoretical model of $\text{Tb}_2\text{Ti}_2\text{O}_7$. The small remaining orientational dependence in T^* , $\mu_0 H_1$, and $\mu_0 H_2$, which corresponds with the magnitude of the magnetization and thus the magnetic anisotropy, provides an important clue in future studies as to what mechanism inhibits the formation of long-range AIAO antiferromagnetism and drives the spin liquid state microscopically.

We thank A. Bauer, P. Böni, C. Franz, B. Gaulin, S. Mayr, R. Moessner, M. Opel, R. Ritz, and A. Regnat for support and stimulating discussions. Financial support through DFG TRR80 and FOR960, the Canadian Institute for Advanced Research (CIFAR), and NSERC is gratefully acknowledged.

-
- [1] J.S. Gardner, M.J.P. Gingras, and J.E. Greedan, *Rev. Mod. Phys.* **82**, 53 (2010).
- [2] S.T. Bramwell and M.J. Gingras, *Science* **294**, 1495 (2001).
- [3] I. Ryzhkin, *JETP* **101**, 481 (2005).
- [4] C. Castelnovo, R. Moessner, and S.L. Sondhi, *Nature (London)* **451**, 42 (2008).
- [5] M.J.P. Gingras, *Introduction to Frustrated Magnetism* (Springer-Verlag, Berlin, 2011).
- [6] H.R. Molavian, M.J.P. Gingras, and B. Canals, *Phys. Rev. Lett.* **98**, 157204 (2007).
- [7] H.R. Molavian, P.A. McClarty, and M.J.P. Gingras, *arXiv:0912.2957*.
- [8] H.R. Molavian and M.J.P. Gingras, *J. Phys. Condens. Matter* **21**, 172201 (2009).
- [9] T. Sakakibara, T. Tayama, Z. Hiroi, K. Matsuhira, and S. Takagi, *Phys. Rev. Lett.* **90**, 207205 (2003).
- [10] O.A. Petrenko, M.R. Lees, and G. Balakrishnan, *Phys. Rev. B* **68**, 012406 (2003).
- [11] O.A. Petrenko, M.R. Lees, and G. Balakrishnan, *J. Phys. Condens. Matter* **23**, 164218 (2011).
- [12] C. Krey, S. Legl, S.R. Dunsiger, M. Meven, J.S. Gardner, J.M. Roper, and C. Pfleiderer, *Phys. Rev. Lett.* **108**, 257204 (2012).
- [13] J.A. Hodges *et al.*, *Phys. Rev. Lett.* **88**, 077204 (2002); K.A. Ross, L. Savary, B.D. Gaulin, and L. Balents, *Phys. Rev. X* **1**, 021002 (2011).
- [14] SungBin Lee *et al.*, *arXiv:1204.2262*.
- [15] J.S. Gardner *et al.*, *Phys. Rev. Lett.* **82**, 1012 (1999).
- [16] I. Mirebeau, P. Bonville, and M. Hennion, *Phys. Rev. B* **76**, 184436 (2007).
- [17] M.J.P. Gingras, B.C. den Hertog, M. Faucher, J.S. Gardner, S.R. Dunsiger, L.J. Chang, B.D. Gaulin, N.P. Raju, and J.E. Greedan, *Phys. Rev. B* **62**, 6496 (2000).
- [18] B.C. den Hertog and M.J.P. Gingras, *Phys. Rev. Lett.* **84**, 3430 (2000).
- [19] S.R. Dunsiger *et al.*, *Physica (Amsterdam)* **326B**, 475 (2003).
- [20] J.S. Gardner *et al.*, *Phys. Rev. B* **68**, 180401 (2003).
- [21] J.S. Gardner, G. Ehlers, S.T. Bramwell, and B.D. Gaulin, *J. Phys. Condens. Matter* **16**, S643 (2004).
- [22] J.P.C. Ruff, B.D. Gaulin, J.P. Castellan, K.C. Rule, J.P. Clancy, J. Rodriguez, and H.A. Dabkowska, *Phys. Rev. Lett.* **99**, 237202 (2007).
- [23] A. Yaouanc *et al.*, *Phys. Rev. B* **84**, 184403 (2011).
- [24] Y. Chapuis, A. Yaouanc, P. Dalmas de Réotier, C. Marin, S. Vanishri, S.H. Curnoe, C. Vâju, and A. Forget, *Phys. Rev. B* **82**, 100402 (2010).
- [25] P. Bonville, I. Mirebeau, A. Gukasov, S. Petit, and J. Robert, *Phys. Rev. B* **84**, 184409 (2011).
- [26] B.D. Gaulin, J.S. Gardner, P.A. McClarty, and M.J.P. Gingras, *Phys. Rev. B* **84**, 140402 (2011).
- [27] G. Luo, S.T. Hess, and L.R. Corruccini, *Phys. Lett. A* **291**, 306 (2001).
- [28] Y. Yasui, M. Kanada, M. Ito, H. Harashina, M. Sato, H. Okumura, K. Kakurai, and H. Kadowaki, *J. Phys. Soc. Jpn.* **71**, 599 (2002).
- [29] N. Hamaguchi, T. Matsushita, N. Wada, Y. Yasui, and M. Sato, *Phys. Rev. B* **69**, 132413 (2004).
- [30] K.C. Rule *et al.*, *Phys. Rev. Lett.* **96**, 177201 (2006).
- [31] H. Cao, A. Gukasov, I. Mirebeau, P. Bonville, and G. Dhalenne, *Phys. Rev. Lett.* **101**, 196402 (2008).
- [32] A. Gukasov, H. Cao, I. Mirebeau, and P. Bonville, *Physica (Amsterdam)* **404B**, 2509 (2009).
- [33] A.P. Sazonov, A. Gukasov, I. Mirebeau, H. Cao, P. Bonville, B. Grenier, and G. Dhalenne, *Phys. Rev. B* **82**, 174406 (2010).
- [34] Y. Yasui, M. Kanada, H. Harashina, M. Sato, H. Okumura, and K. Kakurai, *J. Phys. Chem. Solids* **62**, 343 (2001).
- [35] I. Aleksandrov, B. Lidskii, L.G. Mamsurova, M.G. Neigauz, K.S. Pigalskii, K.K. Pukhov, N.G. Trusevich, and L.G. Scherbakova, *Sov. Phys. JETP* **62**, 1287 (1985).
- [36] L.G. Mamsurova, K.S. Pigalskii, and K.K. Pukhov, *Sov. Phys. JETP* **43**, 755 (1986).
- [37] I. Mirebeau, I.N. Goncharenko, P. Cadavez-Peres, S.T. Bramwell, M.J.P. Gingras, and J.S. Gardner, *Nature (London)* **420**, 54 (2002).
- [38] P.J. Baker, M.J. Matthews, S.R. Giblin, P. Schiffer, C. Baines, and D. Prabhakaran, *arXiv:1105.2196*.
- [39] E. Lhotel, C. Paulsen, P.D. de Réotier, A. Yaouanc, C. Marin, and S. Vanishri, *arXiv:1201.0859*.
- [40] S. Legl, C. Pfleiderer, and K. Krämer, *Rev. Sci. Instrum.* **81**, 043911 (2010).
- [41] S. Legl, Ph.D. thesis, Technische Universität München, 2010.
- [42] J.S. Gardner, B.D. Gaulin, and D.M. Paul, *J. Cryst. Growth* **191**, 740 (1998).
- [43] N. Hamaguchi, T. Matsushita, N. Wada, Y. Yasui, and M. Sato, *J. Magn. Magn. Mater.* **272**, E1007 (2004).
- [44] Y. Chapuis, Ph.D. thesis, Université Joseph Fourier, Grenoble, 2009.
- [45] S.H. Lee, C. Broholm, T.H. Kim, W. Ratcliff, and S.W. Cheong, *Phys. Rev. Lett.* **84**, 3718 (2000).
- [46] O.A. Petrenko, C. Ritter, M. Yethiraj, and D. McK Paul, *Phys. Rev. Lett.* **80**, 4570 (1998).
- [47] See Supplemental Material at <http://link.aps.org/supplemental/10.1103/PhysRevLett.109.047201> for a detailed comparison of the zfc and fc magnetization.
- [48] P.A. McClarty, P. Stasiak, and M.J.P. Gingras, *arXiv:1011.6346*.
- [49] Michael Hermele, Matthew P.A. Fisher, and Leon Balents, *Phys. Rev. B* **69**, 064404 (2004).